

NPCNet: Navigator-Driven Pseudo Text for Deep Clustering of Early Sepsis Phenotyping

Pi-Ju Tsai¹, Charkkri Limbud², Kuan-Fu Chen^{3,4*}, Yi-Ju Tseng^{5,6*}

¹Institute of Data Science and Engineering, National Yang Ming Chiao Tung University, Hsinchu, Taiwan.

²EECS International Graduate Program, National Yang Ming Chiao Tung University, Hsinchu, Taiwan.

³College of Intelligent Computing, Chang Gung University, Taoyuan, Taiwan.

⁴Department of Emergency Medicine, Chang Gung Memorial Hospital, Keelung, Taiwan.

⁵Department of Computer Science, National Yang Ming Chiao Tung University, 1001 University Road, Hsinchu, 300093, Taiwan.

⁶Computational Health Informatics Program, Boston Children's Hospital, Boston, MA, USA.

*Corresponding author(s). E-mail(s): drkfchen@gmail.com;
yjtseng@nycu.edu.tw;

Contributing authors: pjt.cs12@nycu.edu.tw;
charkkri.ee12@nycu.edu.tw;

Abstract

Sepsis is a heterogeneous syndrome. Identifying clinically distinct phenotypes may enable more precise treatment strategies. In recent years, many researchers have applied clustering algorithms to sepsis patients. However, the clustering process rarely incorporates clinical relevance, potentially limiting to reflect clinically distinct phenotypes. We propose NPCNet, a novel deep clustering network with a target navigator that integrates temporal Electronic Health Records (EHRs) to better align sepsis phenotypes with clinical significance. We identify four sepsis phenotypes (α , β , γ , and δ) with divergence in SOFA trajectories. Notably, while α and δ phenotypes both show severe conditions in the early stage, NPC-Net effectively differentiates patients who are likely to improve (α) from those at risk of deterioration (δ). Furthermore, through the treatment effect analysis, we

discover that α , β , and δ phenotypes may benefit from early vasopressor administration. The results show that NPCNet enhances precision treatment strategies by uncovering clinically distinct phenotypes.

1 Introduction

Sepsis is a life-threatening condition that occurs when the body's immune system has an extreme response to an infection that causes organ dysfunction [1]. There are 11 million sepsis-relevant deaths worldwide annually, representing 20% of all global deaths, while survivors often face poor long-term outcomes [2][3]. Activation of timely interventions is critical to improving clinical outcomes [4][5]. For patients with sepsis, each hour of treatment delay has been relevant with a 4–8% increase in risk of death [6].

However, the progression of sepsis varies widely depending on host factors, infection etiology, or the involvement of multiple organ dysfunctions. The inherent heterogeneity dictates that a uniform therapeutic strategy is unlikely to be effective for all patients [7]. Consequently, providing patient-specific care by synthesizing information from multiple sources becomes imperative, yet the primary barrier to this approach is the difficulty of identifying clinically meaningful patterns within complex and temporal electronic health records (EHRs).

To address the heterogeneity of treatment effectiveness, previous studies have employed clustering algorithms to explore distinct sepsis phenotypes [8][9][10]. Such efforts suggest that stratifying patients into subgroups may enable precision medicine approaches [7]. However, most existing approaches consider tabular or regular time series with feature aggregation as the features, overlooking the measurement frequencies of variables, which may reflect severe conditions [11][12]. Moreover, imputation was usually applied to handle missing values, yet it may introduce systematic bias [11][13]. Also, current clustering algorithms rarely consider mechanisms for incorporating knowledge that can reveal clinical significance, such as important clinical outcomes [14][15]. Accordingly, the phenotypes may fail to align with clinical significance, thereby limiting their worth in clinical scenarios.

To advance the development of precision treatment strategies, we propose a novel clustering framework, NPCNet, to identify clinically meaningful sepsis phenotypes. NPCNet employs a text embedding generator that transforms patients' temporal EHRs into pseudo texts, then integrates them with static variables to construct the embeddings. Afterwards, these embeddings learn clinical relevance through two auxiliary tasks by the target navigator component. Finally, by incorporating a clustering operator, NPCNet effectively uncovers four distinct sepsis phenotypes. Fig. 1 summarizes our framework.

We assessed the sepsis phenotypes from three complementary perspectives in the development (MIMIC-IV) cohort. First, NPCNet consistently outperformed existing clustering algorithms in three internal metrics. Second, the identified phenotypes demonstrated clear clinical relevance. Third, treatment effect analysis revealed three

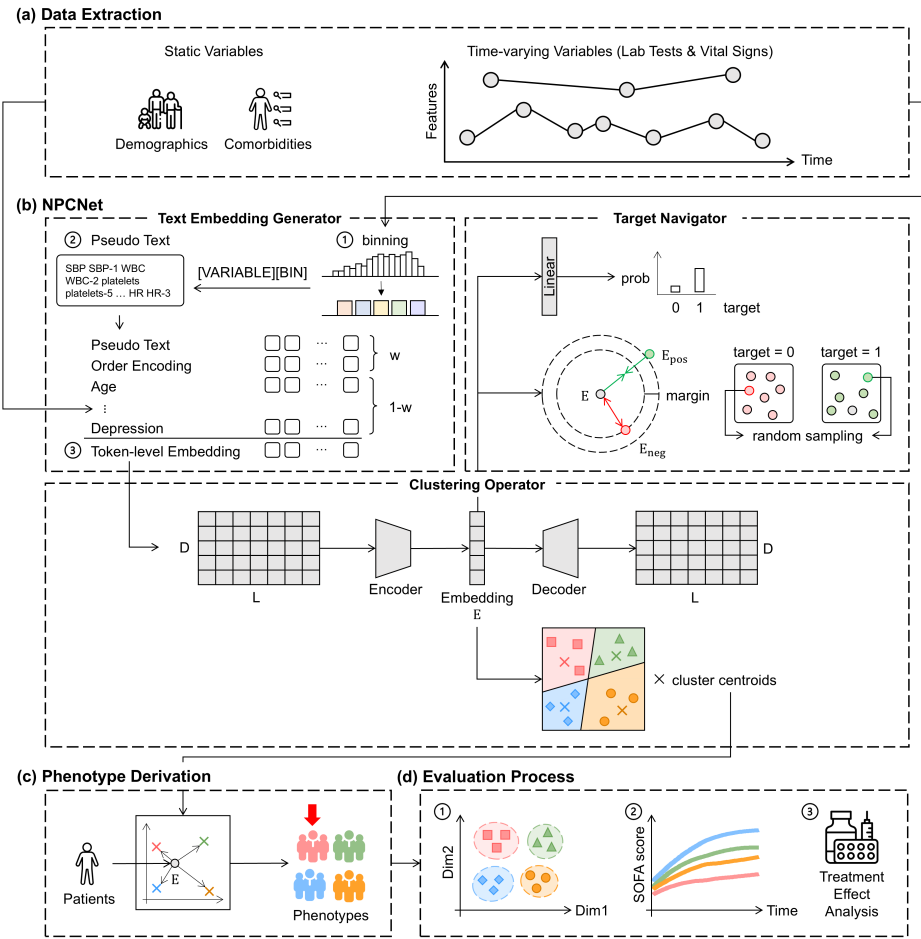


Fig. 1 The overview of the study pipeline. **a** Data extraction. We use static variables, including demographics and comorbidities, together with time-varying variables, such as laboratory test results and vital signs, as the model input. **b** NPCNet architecture. Through the text embedding generator, we first bin the value of time-varying variables into bin indices according to the distribution of the training set. We then transform the series of time-varying variables into pseudo texts, combining static information. NPCNet trains with an objective function that consists of \mathcal{L}_{rec} , $\mathcal{L}_{\text{clustering}}$, and $\mathcal{L}_{\text{navigator}}$. Through the clustering network in the clustering operator and clinical relevance through the target navigator, we can derive the patient embeddings and the centroids of computable phenotypes during the training stage. **c** Phenotype derivation. We only use the information within the first six hours of ICU admission, without the target navigator, to get the patient embeddings. At last, we compute the distance between the patient embeddings and the centroids of phenotypes in the embedding space. Finally, we assign the patients to the nearest phenotypes for further evaluations. **d** Evaluation process. We assess the clustering results from three perspectives: (1) internal evaluation, (2) clinical significance, and (3) treatment effect analysis.

phenotypes that may benefit from early vasopressor administration to varying degrees, highlighting the potential of phenotype-specific treatment strategies. The clustering results were further supported by external validation. Overall, NPCNet provides a framework that bridges computable phenotypes with actionable clinical insights, offering a path to precision treatment strategies.

2 Results

2.1 Cohort characteristics of sepsis phenotypes

The clustering results identified four computable phenotypes of α , β , γ , and δ . The clinical characteristics of each phenotype in the full development cohort appear in **Table 1** and **Supplementary Table 1**. These clinical variables were grouped into eight organ systems, which were inflammatory, pulmonary, cardiovascular, renal, hepatic, hematologic, neurologic, and other systems (**Supplementary Table 2**). The α phenotype was younger with few comorbidities, while the δ phenotype was likely older with more comorbidities (p -values < 0.001). Despite these differences, both α and δ phenotypes demonstrated abnormalities in almost all organ systems, especially in hepatic and hematologic systems, indicating severe conditions at the time of early ICU admission. These observations were based on laboratory measurements where each phenotype showed deviation from the overall medians (**Fig. 2** [16][8]). The β phenotype exhibited abnormalities mainly in the inflammatory and other systems, with few abnormal variables in the remaining organ systems. The γ phenotype was more likely to have elevated inflammatory markers (such as CRP and neutrophils) and renal dysfunction.

Notably, although both α and δ phenotypes exhibited abnormalities in multiple systems (**Fig. 2**), their clinical outcomes differed substantially (**Table 1**). The α phenotype had the lowest in-hospital mortality rate at 1.4%, whereas the δ phenotype showed the highest at 46.2%. When considering 365-day outpatient mortality together, approximately 70.3% of patients in the δ phenotype eventually died. The δ phenotype also had the longest ICU stay, with a median duration of 4.8 days.

2.2 Treatment effects across sepsis phenotypes

The median volume of cumulative intravenous (IV) fluids within 12 hours after initial hypotension was 2.49 liters (IQR, 1.33-4.14), and a vasopressor was initiated rapidly after initial hypotension, with more than 70% of patients receiving the vasopressor in less than 1 hour.

IV fluid administration was comparable across phenotypes and only a few patients, especially those with the δ phenotype, received higher volumes. The time to vasopressor in the α phenotype was earlier than in other phenotypes, while patients in the β and γ phenotypes usually experienced a longer time to vasopressor (**Supplementary Fig. 1**).

The results of multivariable logistic regression in **Fig. 3** showed that, in all phenotypes, there was no statistically significant association between volume of IV fluids and in-hospital mortality. However, the time to vasopressor exhibited phenotype-specific

Table 1 Characteristics of the 4 sepsis computable phenotypes.

Characteristic	Total	α	β	γ	δ
No. of patients (%)	19834 (100)	4624 (23.3)	6246 (31.5)	6250 (31.5)	2714 (13.7)
Age, mean (SD)	64.7 (15.8)	63.3 (14.2)	63.6 (16.2)	66.2 (16.1)	66.1 (16.3)
Sex, No. (%)					
Male	11763 (59.3)	3122 (67.5)	3535 (56.6)	3513 (56.2)	1593 (58.7)
Female	8071 (40.7)	1502 (32.5)	2711 (43.4)	2737 (43.8)	1121 (41.3)
SOFA score, median (IQR)	7 [4, 10]	7 [3, 9]	5 [3, 8]	7 [5, 10]	11 [8, 14]
Elixhauser comorbidities, median (IQR)	0 [0, 5]	0 [0, 0]	0 [0, 5]	4 [0, 6]	5 [0, 7]
Inflammation					
Temperature, mean (SD)	37.0 (0.9)	36.8 (0.7)	37.1 (0.8)	37.0 (0.8)	36.9 (1.1)
Bands, median (IQR)	3.0 [1.4, 5.6]	2.4 [1.2, 4.4]	3.0 [1.4, 5.4]	3.2 [1.6, 6.0]	4.0 [2.0, 7.4]
CRP, median (IQR)	81 [47, 121]	53 [32, 83]	81 [47, 122]	95 [60, 132]	104 [72, 137]
ESR, median (IQR)	49.0 [36.0, 63.6]	48.8 [37.0, 62.4]	49.0 [35.7, 63.8]	49.2 [35.8, 63.8]	49.0 [35.6, 64.0]
WBC, median (IQR)	12.8 [9.2, 17.3]	13.0 [9.7, 16.7]	12.1 [8.7, 16.3]	12.9 [9.1, 17.6]	14.4 [9.9, 20.0]
Neutrophils, median (IQR)	81.3 [75.0, 86.4]	79.3 [74.2, 83.5]	81.3 [74.7, 86.3]	82.5 [75.9, 87.8]	83.0 [75.8, 88.2]
Metamyelocytes, median (IQR)	0.4 [0.2, 1.0]	0.4 [0.2, 0.8]	0.4 [0.2, 1.0]	0.4 [0.0, 1.0]	0.8 [0.2, 1.6]
Myelocytes, median (IQR)	0.2 [0.0, 0.4]	0.2 [0.0, 0.4]	0.2 [0.0, 0.4]	0.0 [0.0, 0.4]	0.2 [0.0, 0.6]
Promyelocytes, median (IQR)	1.2 [1.0, 1.6]	1.2 [1.0, 1.6]	1.2 [1.0, 1.6]	1.2 [1.0, 1.6]	1.2 [1.0, 1.6]
Lymphocytes, median (IQR)	11.0 [7.0, 16.4]	14.5 [10.5, 19.0]	11.1 [7.2, 16.3]	9.3 [5.6, 14.0]	8.7 [5.0, 13.7]
Pulmonary					
SaO ₂ , median (IQR)	84.2 [73.8, 93.0]	86.2 [76.8, 94.6]	84.6 [74.7, 92.4]	83.8 [72.0, 92.4]	81.0 [67.0, 92.0]
PO ₂ , mean (SD)	101 (75)	142 (80)	97 (69)	85 (66)	78 (68)
FiO ₂ , mean (SD)	76.5 (21.9)	85.2 (20.0)	73.0 (20.7)	72.9 (21.9)	77.9 (23.5)
Respiratory rate, mean (SD)	25.2 (7.6)	21.6 (6.6)	24.8 (7.0)	26.7 (7.4)	28.9 (7.9)
Cardiovascular					
Bicarbonate, mean (SD)	21.8 (5.3)	23.1 (3.3)	22.5 (5.0)	21.5 (5.7)	18.4 (6.2)
Heart rate, mean (SD)	98 (21)	91 (15)	97 (20)	101 (22)	106 (24)
Lactate, median (IQR)	2.3 [1.6, 3.5]	2.3 [1.7, 2.9]	2.1 [1.5, 3.0]	2.4 [1.6, 3.6]	3.8 [2.2, 7.3]
SBP, median (IQR)	94 [85, 107]	96 [87, 106]	97 [87, 110]	93 [83, 106]	89 [78, 100]
Troponin, median (IQR)	0.2 [0.1, 0.4]	0.2 [0.1, 0.5]	0.2 [0.1, 0.4]	0.2 [0.1, 0.4]	0.2 [0.1, 0.6]
Renal					
BUN, median (IQR)	24 [16, 40]	17 [13, 22]	22 [15, 35]	32 [19, 50]	36 [23, 56]
Creatinine, median (IQR)	1.2 [0.8, 2.0]	0.9 [0.7, 1.1]	1.1 [0.8, 1.7]	1.4 [1.0, 2.4]	1.8 [1.2, 2.8]
Hepatic					
AST, median (IQR)	66 [36, 143]	72 [43, 136]	60 [33, 128]	61 [32, 133]	92 [41, 293]
ALT, median (IQR)	42 [24, 92]	46 [28, 89]	40 [22, 85]	39 [21, 85]	53 [25, 167]
Bilirubin, median (IQR)	0.9 [0.5, 1.7]	0.9 [0.6, 1.5]	0.9 [0.5, 1.8]	0.8 [0.5, 1.8]	0.9 [0.5, 1.9]
Hematologic					
Hemoglobin, mean (SD)	10.1 (2.4)	9.5 (2.1)	10.2 (2.3)	10.3 (2.4)	10.3 (2.6)
INR, median (IQR)	1.4 [1.2, 1.7]	1.3 [1.2, 1.5]	1.3 [1.2, 1.6]	1.4 [1.2, 1.8]	1.6 [1.2, 2.4]
Platelets, median (IQR)	174 [120, 241]	155 [119, 202]	182 [126, 253]	187 [123, 256]	172 [102, 247]
Neurologic					
GCS, mean (SD)	9.2 (4.9)	7.3 (5.0)	10.8 (4.6)	9.9 (4.6)	7.0 (4.4)
Others					
Albumin, mean (SD)	3.2 (0.5)	3.2 (0.5)	3.2 (0.5)	3.2 (0.6)	3.1 (0.6)
Chloride, mean (SD)	105 (7)	108 (5)	104 (7)	104 (8)	105 (9)
Glucose, median (IQR)	154 [121, 200]	162 [136, 190]	145 [115, 192]	149 [116, 202]	174 [128, 250]
Sodium, mean (SD)	139 (6)	140 (3)	139 (5)	139 (7)	140 (7)
Outcomes					
In-hospital mortality, No. (%)	3159 (15.9)	64 (1.4)	508 (8.1)	1332 (21.3)	1255 (46.2)
365-day outpatient mortality, No. (%)	5355 (27.0)	597 (12.9)	1918 (30.7)	2185 (35.0)	655 (24.1)
Length of stay in the ICU, median (IQR)	3.0 [1.8, 5.9]	2.1 [1.3, 3.3]	2.8 [1.8, 5.3]	3.8 [2.2, 7.2]	4.8 [2.6, 9.3]
Length of stay in the hospital, median (IQR)	8.3 [5.2, 14.4]	6.5 [5.0, 10.0]	8.5 [5.4, 14.5]	9.8 [5.9, 16.7]	9.6 [4.5, 17.0]
Day of mechanical ventilation, median (IQR)	2.08 [0.93, 4.83]	1.29 [0.80, 2.67]	1.83 [0.80, 4.25]	2.72 [1.21, 6.04]	3.88 [1.69, 8.26]
Volume of IV fluids (L), median (IQR)	4.7 [2.4, 9.5]	3.8 [2.4, 6.0]	4.3 [2.0, 8.6]	5.4 [2.3, 11.3]	8.0 [3.9, 15.4]
Administration of a vasopressor, No. (%)					
Dopamine	948 (4.8)	79 (1.7)	213 (3.4)	387 (6.2)	269 (9.9)
Phenylephrine	6303 (31.8)	2492 (53.9)	1465 (23.5)	1418 (22.7)	928 (34.2)
Norepinephrine	7450 (37.6)	707 (15.3)	1967 (31.5)	2916 (46.7)	1860 (68.5)
Vasopressin	2475 (12.5)	176 (3.8)	455 (7.3)	901 (14.4)	943 (34.7)
Epinephrine	1553 (7.8)	542 (11.7)	365 (5.8)	289 (4.6)	357 (13.2)
Dobutamine	525 (2.6)	18 (0.4)	86 (1.4)	219 (3.5)	202 (7.4)

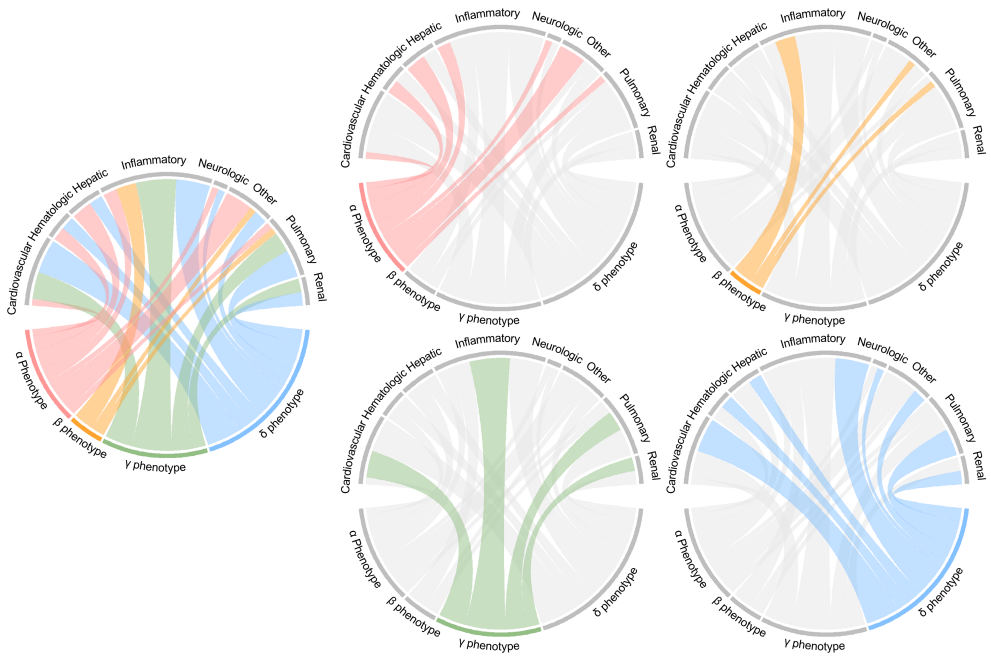


Fig. 2 Abnormal clinical variables, grouped into eight organ systems, among the sepsis computable phenotypes. The ribbon connects from a phenotype to an organ system if the group median is more abnormal than the overall median (Supplementary Table 2). The more clinical variables are abnormal for the phenotype, the broader the ribbon.

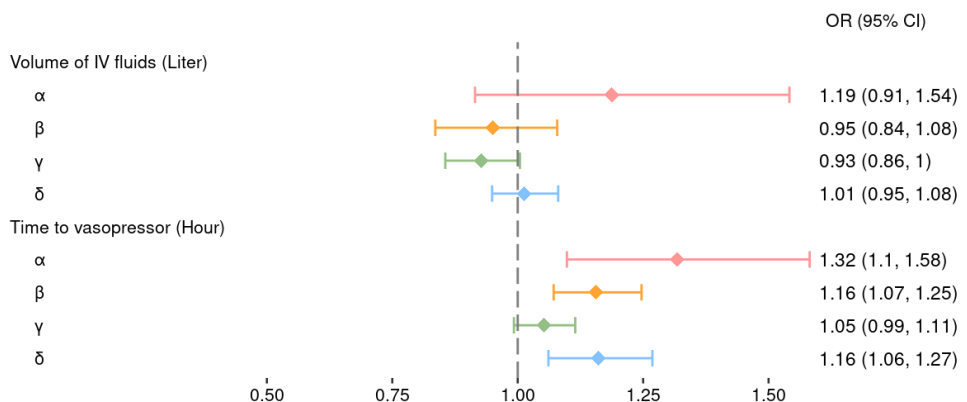


Fig. 3 Multivariable logistic regression on in-hospital mortality with phenotypes.

effects. A one-hour delay in the time to vasopressor initiation was associated with a 31.8% increase in the odds of in-hospital mortality for patients with the α phenotype, after adjusting for other variables, such as age and gender, listed in **Supplementary Table 3**. For the β and δ phenotypes, the corresponding increase was 15.6% and 16.0%, respectively, while no statistically significant association was observed for the γ phenotype.

2.3 Sensitivity analysis of treatment effects

For the α phenotype, the approximate E-value [17] for the observed association between time to vasopressor and in-hospital mortality was 1.56, with 1.27 for the lower confidence limit. This indicates that an unmeasured confounder associated with both time to vasopressor and in-hospital mortality, each by an effect size equivalent to a risk ratio of at least 1.56, could explain away the observed effect. The corresponding approximate E-values (and lower limits) for the β and δ phenotypes were 1.36 (1.23) and 1.37 (1.21), respectively, for the observed association between time to vasopressor and in-hospital mortality.

2.4 Internal evaluation of clustering performance

NPCNet significantly outperformed all other models on the three internal metrics (**Table 2**), indicating that the phenotypes were more cohesive with clearer boundaries, thereby yielding more robust embedding structures.

Table 2 The performance of NPCNet and benchmarks in the testing set.

Model	SI \uparrow	CHI \uparrow	DBI \downarrow
consensus K-means [18]	-0.043 (0.011)***	0.040 (0.005)***	5.426 (0.870)***
KM-DTW	0.000 (0.000)***	0.335 (0.004)***	1.993 (0.011)***
DCN [19]	0.344 (0.048)***	1.482 (0.420)**	1.140 (0.083)***
DKM [20]	0.290 (0.053)***	0.423 (0.029)***	1.690 (0.098)***
naviDCN [21]	0.335 (0.076)***	0.824 (0.285)***	1.184 (0.129)***
NPCNet	0.447 (0.012)	2.051 (0.161)	0.670 (0.022)

** $p < 0.01$, *** $p < 0.001$. For each model, we report the average scores over 10 random seeds. The second-best results based on the average scores are underlined.

2.5 Clinical trajectories across sepsis phenotypes

These sepsis phenotypes demonstrated distinct SOFA trajectories across nearly all stratifications, with the severity progressively increasing from the α to the δ phenotype, showing that NPCNet effectively captured the sepsis phenotypes, which have short-term differences in the progression of organ dysfunction (**Fig. 4a**). To further illustrate the distinctiveness of SOFA trajectories across models, we visualized the trajectories within each stratum as heatmaps and quantified their separability using the Trajectory Divergence Index (TDI), which was derived by normalizing the number of statistically

significant pairs by the total number of pairwise comparisons (**Fig. 4b**). NPCNet consistently achieved higher divergence in most stratifications by approximately 10 hours after ICU admission, whereas naviDCN [21] required longer for the phenotypes to demonstrate the divergence. Other models do not exhibit a consistent pattern in divergence over time. Furthermore, NPCNet also revealed distinct long-term outcomes, such as Kaplan-Meier curves of one-year mortality in **Fig. 4c**.

2.6 Ablation study of NPCNet components

To evaluate the contribution of each component in NPCNet, we conducted four ablation studies. First, for the text embedding generator, using binned laboratory values with order encoding outperformed the use of raw laboratory values with timeline encoding (**Supplementary Table 4**). Among different backbones for embedding extraction, NPCNet consistently surpassed both the MLP and CNN autoencoders, highlighting the advantage of preserving temporal information through pseudo-text representations (**Supplementary Table 5**). When comparing loss functions in the target navigator module, the combination of probability and distance losses yielded the best performance (**Supplementary Table 6**). Finally, across all navigator targets, the discharge status navigator produced phenotypes with the greatest differentiation in clinical outcomes (**Supplementary Fig. 2**, **Fig. 3**, **Fig. 4**).

2.7 External validation

We evaluated the generalizability of the sepsis phenotypes identified by NPCNet in the MIMIC-IV cohort using the eICU cohort. Similarly to the clustering results in the MIMIC-IV cohort, both α and δ phenotypes exhibited abnormalities across multiple organ systems (**Supplementary Table 7**, **Supplementary Table 8**, and **Supplementary Fig. 5**), particularly in the hepatic and hematologic systems. Consistent with the findings from MIMIC-IV, these phenotypes were associated with substantially different clinical outcomes (**Supplementary Table 7**). The δ phenotype exhibited increasing SOFA trajectories over time, whereas the α phenotype showed decreasing SOFA trajectories (**Supplementary Fig. 6**). In the treatment effect analysis, neither the volume of IV fluids nor the time to vasopressor showed a statistically significant association with in-hospital mortality across phenotypes (**Supplementary Fig. 7**, **Fig. 8**).

3 Discussion

Existing approaches to sepsis phenotyping faced multiple challenges, such as modeling temporal EHRs or incorporating clinical relevance in the model. NPCNet bridged the gap between three important objectives in sepsis phenotyping: (1) generating representative embeddings; (2) preserving the integrity of phenotypes in the embedding space; and (3) aligning phenotypes with clinical significance. First, NPCNet transformed patients' temporal information into pseudo texts, preserving the intrinsic attributes of EHRs. Then, by integrating the target navigator into the deep clustering network, NPCNet improved the alignment of computable phenotypes with important clinical

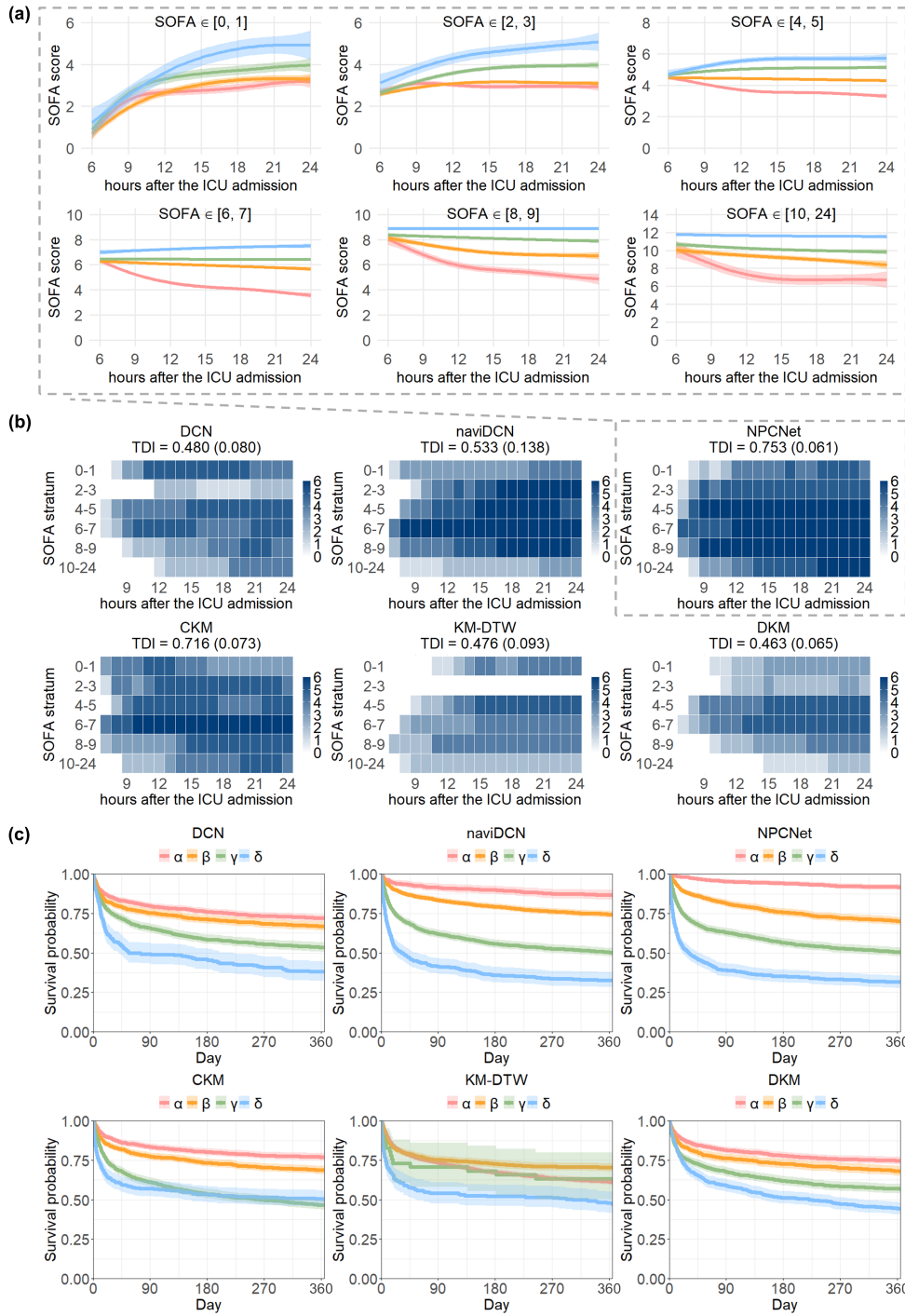


Fig. 4 The clinical outcomes across phenotypes in the testing set. **a** SOFA trajectories during the 18 hours following phenotype derivation by NPCNet, stratified by the SOFA score at six hours after ICU admission. **b** Pairwise comparisons of SOFA trajectories between four phenotypes at each hour within each stratum for NPCNet and benchmarks. The cell in the heatmap represents the number of significantly different phenotype pairs, out of six total possible pairwise combinations, at each time point within each SOFA stratum. The values range from 0 to 6, with darker colors indicating more pairwise differences, thereby reflecting how distinguishable the phenotypes are over time. The Trajectory Divergence Index (TDI) was then derived by normalizing the number of statistically significant pairs by the total number of pairwise comparisons, yielding a metric between 0 and 1 that quantifies the overall performance of models in clinical significance. **c** Kaplan-Meier curves of one-year mortality for the phenotypes derived by NPCNet and benchmark models.

outcomes, while still maintaining the integrity of phenotypes in the embedding space. Extensive ablation studies highlighted that all components contribute to overall performance. Through comparisons with benchmarks, NPCNet demonstrated superior performance in clinical relevance and clustering, showing its ability to mine clinical phenotypes from temporal EHRs.

NPCNet effectively differentiated phenotypes with different SOFA trajectories. Despite initially presenting with comparable SOFA scores within each stratum, the four phenotypes demonstrated a marked divergence in their SOFA trajectories 18 hours later. This highlighted the capability of NPCNet to inform precision treatment strategies. The SOFA score provides a quantitative measure of organ dysfunctions [22]. Prior studies have shown that maximum SOFA scores were strongly relevant to mortality, with even modest changes reflecting significant variations in a patient's prognosis [23]. These phenotypes can represent underlying differences in pathophysiology, allowing the stratification of patients who are more likely to benefit from specific therapeutic interventions [9].

The results of treatment effect analysis showed no statistically significant association between the volume of IV fluids and in-hospital mortality in all phenotypes. Along with the previous study [24], these observations were consistent with the findings in the entire group. There was no statistically significant difference in mortality with conservative or deresuscitative strategies in comparison with a liberal strategy or usual care [25]. These suggest that even after considering the heterogeneity of phenotypes, fluid timing or volume alone may not independently predict in-hospital mortality, highlighting the need for further validation through clinical trials.

In contrast, multivariable logistic regression found that early administration of vasopressors appeared to be relevant to reducing in-hospital mortality among the three phenotypes (α , β , and δ phenotypes). Multiple studies have shown that early vasopressor initiation improves outcomes [26][27][28]. Our phenotype-specific findings had similar results for this recommendation. These findings collectively promote the importance of phenotyping in tailoring treatment strategies.

The phenotypes identified by NPCNet align with and extend previous findings in sepsis research. Consistent with a landmark study that identified four clinically distinct sepsis phenotypes with cross-sectional summaries of early clinical variables [8], our results show comparable profiles. For example, our β phenotype closely resembles the lower-risk α phenotype in [8], with fewer abnormal laboratory values and similar patterns of organ dysfunction involving inflammatory, pulmonary, and other systems. Similarly, our δ phenotype aligns with the high-risk δ phenotype in [8], exhibiting multi-organ dysfunctions. Uniquely, however, NPCNet reveals that the poor outcomes in δ phenotype may persist despite active interventions like vasopressor therapy, highlighting the need for novel therapeutic approaches. While a previous study showed that the time to IV fluid completion was not significantly relevant to in-hospital mortality [24], we extended this to examine the volume of IV fluids administered within 12 hours after initial hypotension. We found no statistically significant association between fluid volume and in-hospital mortality in four phenotypes. Finally, NPCNet demonstrates a significant advantage in clinical timeliness and efficiency. While previous

study [9] required 72-hour SOFA trajectories to provide four sepsis phenotypes, NPC-Net achieves this using data from only the first six hours of ICU admission. NPCNet not only identified four phenotypes with clearly distinguishable trajectory patterns, but also further explored how treatment strategies may differ across phenotypes.

To evaluate generalizability, we applied the model and binning thresholds derived from MIMIC-IV directly to the eICU cohort without re-training. In this external validation setting, the identified phenotypes exhibited similar clinical characteristics, in-hospital mortality, and SOFA trajectory patterns to those observed in the MIMIC-IV cohort. In contrast, treatment-related findings on time to vasopressor were less consistent across cohorts, likely reflecting the known limitation in the eICU cohort, where incomplete documentation, such as drug infusion, has been previously mentioned [29]. Nonetheless, the external validation suggests that the proposed framework is generalizable to other cohorts.

Our study has several limitations. First, NPCNet only relies on commonly available clinical variables. The inclusion of biomarkers or transcriptome variables may provide deeper insights into the pathophysiological mechanisms [7][30]. Additionally, the clinical metric, TDI, currently only evaluates whether the SOFA trajectories of different phenotypes are distinguishable, without considering the level of divergence. Furthermore, the choice of significance level may influence the TDI value. Therefore, further adjustment of TDI is necessary to assess the clinical relevance of phenotypes of different models with more care. Next, this retrospective observational study cannot establish causality regarding whether treatments directly affect outcomes. Moreover, because clinical measurements and interventions are retrospectively documented, their timestamps may not precisely reflect the actual time of clinical events, potentially introducing measurement bias. Finally, the treatment effect analysis only applies to patients who have ever received vasopressors, limiting our ability to evaluate treatment strategies among patients who did not receive them. Nevertheless, the findings provide preliminary evidence that may inform the development of future prospective studies.

4 Methods

4.1 Cohort description

We used the Medical Information Mart for Intensive Care (MIMIC)-IV version 2.2 database as the development cohort [31], which contains patients who have ever been admitted to the emergency department or an intensive care unit at Beth Israel Deaconess Medical Center (BIDMC) in Boston, MA, from 2008 to 2022.

We identified sepsis cases with the definition of Sepsis-3 [32] in every hospitalization's first ICU stay (**Supplementary Fig. 9, Fig. 10**). We excluded sepsis cases with ICU stays of less than 24 hours to ensure that sufficient clinical data were available for analysis. In addition, cases whose sepsis onset occurred more than 24 hours before or after ICU admission were excluded, in order to minimize variability in disease progression and to ensure that the timing of sepsis onset was relatively comparable across individuals. This resulted in 19,834 sepsis episodes for clustering analysis.

After clustering, we further investigated whether different phenotypes exhibit different responses to treatments by focusing on two specific interventions: (1) the volume of IV fluids, (2) time to vasopressor [33][27]. To ensure the suitability of the study population for treatment effect analysis, we applied additional inclusion and exclusion criteria as in **Supplementary Fig. 11**. First, we included cases that received vasopressors. We then excluded cases whose MAP remained above 65 mmHg within one hour after vasopressor initiation [5]. Because vital signs in the cohort were typically recorded at hourly intervals, we applied a one-hour buffer to ensure that episodes of hypotension were captured. In addition, we included those whose initial vasopressor was norepinephrine [5]. Next, to prevent extreme outliers from biasing the model estimation (as more than 80% of the patients had time gaps of less than 12 hours), we excluded cases whose time to vasopressor exceeded 12 hours. Finally, we removed cases with congestive heart failure or renal failure because they may follow different intravenous therapy strategies. After applying all criteria, 2,013 cases remained for treatment effect analysis. For extracting the volume of IV fluids of sepsis cases, we followed the procedures from the previous study [34].

For external validation, we further utilized the eICU Collaborative Research Database [29], a multi-center intensive care database containing de-identified health records from over 200 hospitals across the United States between 2014 and 2015. Sepsis cases in the eICU cohort were identified based on publicly available code from prior work [35]. For treatment effect analysis, the same selection criteria as those applied to the MIMIC-IV cohort were used. Finally, we identified 13,660 cases for clustering analysis (**Supplementary Fig. 12**) and 1,235 cases for treatment effect analysis (**Supplementary Fig. 13**).

4.2 Variable selection

We included 65 variables for the cluster analysis [8], including two demographics, 31 Elixhauser comorbidities, 28 laboratory test results, and four vital signs. To derive the Elixhauser comorbidities index, we used diagnosis codes from prior hospitalizations or emergency department visits. We extracted other variables within the first six hours after admission to the ICU. The details of the variables are presented in **Supplementary Table 2** for the development cohort and **Supplementary Table 9** for the external validation cohort. We set the range of values for each variable [8][35], removed clinical invalid entries (e.g., 999999) that likely indicated missing values or placeholder codes, while retaining only clinically valid values.

4.3 NPCNet architecture

Fig. 1b illustrates the workflow, including the text embedding generator, the clustering operator, and the target navigator. We first extract variables from EHRs. The time-varying variables are then converted into pseudo text by a binning task, with the order of examination. Then, the pseudo text from time-varying variables is stacked with static information and serves as the input of NPCNet. After processing the input to embedding E through the encoder in the clustering operator, we alternately optimize the network weights and the cluster centroids of the phenotypes. While optimizing

the network weights, the target navigator infuses clinical relevance, such as discharge status, into the embedding during backpropagation, guiding the clustering operator with more specific directions in the embedding space.

4.4 Text embedding generator

We extract static and time-varying variables separately and then integrate them to form a token-level embedding (Fig. 1b, upper left). For time-varying variables, we collect vital signs and laboratory tests within the first six hours after ICU admission. Because the tokenization-embedding paradigm does not work well with numerical numbers [36], we apply the binning task before transforming the records into pseudo text. By discretizing the values of each variable into B distinct qualitative bins according to the quantiles of the training set, each bin of each variable contains an equal number of observations. For instance, one examination of Subject 1 was SBP, with a result (value) that falls into the first bin (0th percentile - 10th percentile if $B=10$), and we encoded its value as "SBP-1" (more examples in **Supplementary Fig. 14**). After converting all values into bin indices, we arrange them in the chronological order of examinations using the format [VARIABLE][BIN] to form a pseudo text with length l [37].

To convert pseudo text into token-level embeddings, we first tokenize the pseudo text into tokens, which are split by the space. Let a pseudo text \mathcal{T} be $[w_0, w_1, \dots, w_{l-1}]$, where w_i is the i -th token in the pseudo text of length l . The tokenization process maps each token to an index from a vocabulary \mathcal{V} , yielding \mathcal{I} to be $[t_0, t_1, \dots, t_{l-1}]$, where $t_i \in \mathcal{V}$. We then obtain the token-level embedding $\mathbf{P} \in \mathbb{R}^{l \times d}$ from an embedding matrix $v \in \mathbb{R}^{|\mathcal{V}| \times d}$ that corresponds to the vocabulary \mathcal{V} :

$$\mathbf{P} = [e_0, e_1, \dots, e_{l-1}],$$

where $e_i = v[t_i]$ and d is the embedding dimension.

To incorporate the temporal structure of the time-varying variables, we introduce an order encoding, which is the same as positional encoding in Transformer [38], but corresponds to the examination order of variables here. $\mathbf{O} \in \mathbb{R}^{l \times d}$ is the matrix stacking the order encoding OE of all positions:

$$\mathbf{O} = [\text{OE}_{(0)}, \text{OE}_{(1)}, \dots, \text{OE}_{(l-1)}],$$

For static variables, such as demographics or comorbidities, the values do not change throughout the stay. Therefore, the value for each static variable is the same in every token of pseudo text [39]. We present each category of each variable c_i with an embedding $\in \mathbb{R}^d$ by the embedding matrix E_i for the i -th static variable. For a given patient, we sum the embeddings corresponding to the patient's category across all static variables to derive the static embedding $\mathbf{S} \in \mathbb{R}^d$:

$$\mathbf{S} = \sum_i E_i[c_i].$$

Finally, we sum up (1) the pseudo text embedding \mathbf{P} with order encoding \mathbf{O} , and (2) the static embedding \mathbf{S} using different weights, resulting in the input $x \in \mathbb{R}^{l \times d}$:

$$x = w \times (\mathbf{P} + \mathbf{O}) + (1 - w) \times \mathbf{S},$$

where $w \in [0, 1]$ is a hyperparameter that controls the contribution of static and time-varying variables. The example is shown in **Supplementary Fig. 15**.

By converting the time-varying variables into pseudo text, we can utilize the complete temporal resolution of measurements without imputation or aggregation. When certain variables are missing, they are simply absent from the text, avoiding the potential noise from imputation. Similarly, when multiple measurements exist for the same variable, all are kept in the text, eliminating the requirement for aggregation that may obscure clinically significant fluctuations.

4.5 Clustering operator

We use Deep Clustering Network (DCN) [19] as the clustering operator (**Fig. 1b**, bottom). DCN adopts an alternating stochastic optimization approach that jointly optimizes reconstruction loss \mathcal{L}_{rec} and clustering loss $\mathcal{L}_{\text{clustering}}$.

$$\mathcal{L}_{\text{rec}} = \sum_{i=1}^N \| x_i - \hat{x}_i \|_2^2, \quad (1)$$

where N is the number of patients and \hat{x} is the reconstruction of x from the output of the decoder.

$$\mathcal{L}_{\text{clustering}} = \sum_{i=1}^N \| E_i - M s_i \|_2^2 \quad (2)$$

s.t. $s_{j,i} \in \{0, 1\}$, $\mathbf{1}^T s_i = 1 \forall i, j$,

where $M \in \mathbb{R}^{k \times d}$ is the matrix including clustering centroids, k is the number of clusters, and s_i is the one-hot assignment vector.

4.6 Target navigator

To enhance the clinical relevance of clustering results, we introduce the target navigator. Through applying two auxiliary tasks, the navigator enables the embedding to progressively learn clinical relevance through backpropagation while simultaneously refining the assignment of phenotypes. When the embedding contains more clinical relevance, the clustering results can uncover more heterogeneity among phenotypes.

The target navigator guides the learning of the embedding from two auxiliary tasks, one is that we expect the embedding to learn the knowledge of whether the patient is alive or not at discharge [21]. The other is relevant to relational knowledge by the relative positions of patients in the embedding space. Taking the discharge status navigator for example, we expect patients with the same discharge status to be closer while keeping patients with different discharge statuses away from each other in the embedding space, guiding the embedding to align with clinically meaningful differences.

First, the embedding is passed through a linear layer, followed by a softmax activation to output the probabilities for each discharge status.

$$p = \text{softmax}(W^T E + b), \quad (3)$$

where $W \in \mathbb{R}^{d \times c}$ and $b \in \mathbb{R}^c$ are learnable parameters, and c is the number of categories. By comparing these probabilities with the actual clinical status y , the probability loss is as follows:

$$\begin{aligned} \mathcal{L}_{\text{prob}} &= -\frac{1}{N} \sum_{j=1}^N \sum_{i=1}^c w_i (1 - p_{t,i}^j)^\gamma \log(p_{t,i}^j), \\ p_{t,i}^j &= \begin{cases} p_i^j & \text{if } y^j = i \\ 1 - p_i^j & \text{otherwise,} \end{cases} \end{aligned} \quad (4)$$

where w_i is the weight hyperparameter, p_i is the probability of discharge status i , and γ is the hyperparameter representing the modulating factor. w_i addresses class imbalance by weighting each discharge status with reference to its proportion. γ controls the contribution of each patient. For patients whose probabilities for each status are close to each other, the contribution to $\mathcal{L}_{\text{prob}}$ is larger. The value is lower for the patient with a high probability of a certain discharge status, thus encouraging the model to focus more on challenging ones.

Then, the model adopts a triplet strategy. For each anchor (a), we randomly sample (1) a positive sample (p) with the same discharge status as the anchor, and (2) a negative sample (n) with a different discharge status, both drawn from the training set. By computing the Euclidean distances among these samples, the distance loss aims to minimize the distance between patients of the same discharge status while maximizing the distance between those with different categories. This helps to ensure that the embedding not only represents the clinical characteristics of patients but also encodes key clinical relevance, clustering patients with similar statuses more closely.

$$\mathcal{L}_{\text{dist}} = \max(d(a, p) - d(a, n) + \text{margin}, 0) \quad (5)$$

where $d(\cdot, \cdot)$ is the Euclidean distance, then margin is a hyperparameter to control the minimum separation between samples with different categories. If the difference in distances does not surpass the margin, the distance loss is set to zero, indicating that the objective has been met enough.

The overall target navigator loss is the sum of two losses with different weights:

$$\mathcal{L}_{\text{navigator}} = \kappa_1 * \mathcal{L}_{\text{prob}} + \kappa_2 * \mathcal{L}_{\text{dist}}, \quad (6)$$

where κ_1 and κ_2 are hyperparameters.

Ultimately, the overall loss function of NPCNet is as follows:

$$\mathcal{L} = \lambda_1 * \mathcal{L}_{\text{rec}} + \lambda_2 * \mathcal{L}_{\text{clustering}} + \lambda_3 * \mathcal{L}_{\text{navigator}}, \quad (7)$$

where λ_1 , λ_2 , and λ_3 are hyperparameters to balance three components. Then, we leverage \mathcal{L} as the overall objective to adjust the network weights during backpropagation.

4.7 Clinical significance analysis

To objectively assess the clinical relevance of the phenotypes of different clustering models, we evaluate whether patients with different phenotypes exhibit distinguishable progression patterns of short-term deterioration of organ dysfunction. Specifically, for each patient, we compute the hourly SOFA score from 7 to 24 hours after ICU admission. This results in SOFA trajectories to quantify the progression of organ failure across phenotypes.

We first stratify patients into six groups according to their SOFA scores at the sixth hour after ICU admission to reduce the confounding effect of patients' initial severity on the comparisons. These subgroups are taken from the relationships between early SOFA scores and mortality as follows: [0, 1], [2, 3], [4, 5], [6, 7], [8, 9], and [10, 24] [40].

Within each stratum, we compare the SOFA trajectories of all cluster pairs using Generalized Additive Mixed Model (GAMM). GAMM allows for flexible modeling of non-linear time-dependent patterns among phenotypes while considering the variability across patients. Next, we introduce the Trajectory Divergence Index (TDI) according to GAMM to quantify the performance in the clinical relevance of different clustering models. For each hourly time point, we test whether the SOFA trajectories differ significantly between phenotypes. We perform this comparison pairwise for all phenotypes, within each stratum, and for each hourly window from the 7th to the 24th hour after ICU admission. For example, with four phenotypes, there are six cluster pairs per stratum, 18 time points, resulting in a total of 648 pairwise comparisons.

$$TDI = \frac{\text{the number of statistically significant pairs}}{\text{the number of pairwise comparisons}} \quad (8)$$

We normalize the number of statistically significant pairs by dividing by the number of pairwise comparisons, yielding a metric ranging from 0 to 1 that reflects the model's ability to produce phenotypes that have different short-term SOFA trajectories.

4.8 Treatment effect analysis

In addition to examining clinical outcomes such as mortality within each phenotype, we also aim to investigate whether the treatment effects vary across phenotypes. Specifically, we employ multivariable logistic regression to assess whether the phenotypes modify the relationship between (1) the volume of IV fluids, defined as the cumulative fluid input within 12 hours after initial hypotension (MAP \downarrow 65), and (2) the time to vasopressor, defined as the duration from initial hypotension to vasopressor initiation, with in-hospital mortality. **Supplementary Table 3** provides descriptions of the variables in the logistic regression.

Finally, for each phenotype, we examine the corresponding coefficient of each treatment term by the Wald test. If the p -value is less than the significance level, the treatment is thought to have a statistically significant association with in-hospital

mortality. By comparing the treatment effects across phenotypes, we aim to determine whether phenotypes moderate the impact of treatment on in-hospital mortality.

4.9 Sensitivity analysis of treatment effects

To assess the robustness of the observed associations between treatment effects and in-hospital mortality in each sepsis phenotype to potential unmeasured confounders, we conducted a sensitivity analysis using the E-value [17]. The E-value represents the minimum strength of an unmeasured confounder’s association with both the exposure and outcome that would be required to fully explain away the observed effect estimate, expressed on the risk ratio scale. We calculated the E-value and its lower confidence limit based on the odds ratio (OR) and its 95% confidence interval.

4.10 Implementation details

To prevent data leakage due to the target navigator, the MIMIC-IV cohort was split by patients, as individual patients could contribute multiple episodes. The MIMIC-IV cohort was divided into a training set (80%) and a testing set (20%). Thresholds for the binning task were derived exclusively from the training set and subsequently applied to the testing set. During the training stage, the target navigator was incorporated to guide the model to learn clinical knowledge, whereas in the testing stage, the navigator was removed, and model inputs were restricted to information from the first six hours after ICU admission. The eICU cohort served as the external validation cohort. To assess the model’s generalizability and robustness across different cohorts, the binning thresholds and trained model derived from the MIMIC-IV training set were directly applied to the eICU cohort without re-training.

Following the previous studies [8][9][33], we set four as the number of phenotypes. We use the random search to choose the hyperparameters. The details of the model settings are shown in **Supplementary Table 10**. The clinical characteristics of the training and the testing sets are in **Supplementary Table 11**. There were no statistically significant differences in almost all the variables between the two subsets. Each experiment was run 10 times with different random seeds to ensure the robustness of the results. All the comparisons of NPCNet with benchmarks or ablation studies used the same testing set to maintain consistency across evaluations.

For the evaluation of clustering algorithms, performance metrics consisted of external and internal metrics. Since sepsis phenotypes lack a universal definition, this study exclusively focused on internal metrics, which objectively assess the clustering results. Internal metrics focus on (1) the compactness within a cluster and (2) the separation between clusters. We chose three common internal metrics, the Silhouette Index (SI), the Calinski-Harabasz Index (CHI), and the Davies-Bouldin Index (DBI). Higher SI and CHI values, alongside a lower DBI, indicate better clustering quality. Additionally, to assess clinical relevance, we designed a clinical metric, TDI, that demonstrates the model’s ability to produce phenotypes that can identify short-term organ failure trajectories, ranging from 0 to 1.

4.11 Statistical analysis

When presenting the clinical characteristics of the sepsis phenotypes, we reported the mean (SD) for quantitative variables. Unless the variables had higher skewness, we substituted them with the median (IQR). Qualitative variables were presented by the number (%). For comparisons between different subsets, we used the t-test or the Mann-Whitney U test for continuous variables, while using the chi-square test for qualitative variables. When comparing two different clustering models, we used a two-sample t-test to test statistical significance. The significance level was set to 0.05 for statistical significance.

5 Data availability

MIMIC-IV is available from <https://physionet.org/content/mimiciv/2.2/>. The eICU Collaborative Research Database is publicly available at <https://physionet.org/content/eicu-crd/2.0/>.

6 Code availability

The source code for the proposed NPCNet framework is available at <https://github.com/DHLab-TSENG/NPCNet>.

7 Acknowledgments

This study was supported by grants from the National Science and Technology Council, Taiwan (NSTC 114-2221-E-A49-061 and 114-2634-F-A49-006), the CGMH-NYCU Joint Research Program (CGMH-NYCU-114-CORPG2P0072), and Chang Gung Memorial Hospital (CMRPG2P0342). The funders had no role in the study design and procedures; data collection, management, analysis, and interpretation; manuscript preparation, review, and approval; or the decision to submit the manuscript for publication.

8 Author contributions

PJT had full access to all the data in the study and takes responsibility for the integrity of the data and the accuracy of the data analysis. PJT conducted the experiments and analyzed/interpreted the data. PJT and YJT designed the study and drafted the manuscript. CL and KFC reviewed/edited the manuscript for important intellectual content and provided administrative, technical, or material support. YJT and KFC obtained funding and supervised the study.

9 Competing interests

The authors have no competing interests to declare.

References

- [1] Singer, M., Deutschman, C.S., Seymour, C.W., Shankar-Hari, M., Annane, D., Bauer, M., Bellomo, R., Bernard, G.R., Chiche, J.-D., Coopersmith, C.M., *et al.*: The third international consensus definitions for sepsis and septic shock (sepsis-3). *Jama* **315**(8), 801–810 (2016)
- [2] Rudd, K.E., Johnson, S.C., Agesa, K.M., Shackelford, K.A., Tsoi, D., Kievlan, D.R., Colombara, D.V., Ikuta, K.S., Kissoon, N., Finfer, S., *et al.*: Global, regional, and national sepsis incidence and mortality, 1990–2017: analysis for the global burden of disease study. *The Lancet* **395**(10219), 200–211 (2020)
- [3] Prescott, H.C., Iwashyna, T.J., Blackwood, B., Calandra, T., Chlan, L.L., Choong, K., Connolly, B., Dark, P., Ferrucci, L., Finfer, S., *et al.*: Understanding and enhancing sepsis survivorship. priorities for research and practice. *American journal of respiratory and critical care medicine* **200**(8), 972–981 (2019)
- [4] Prescott, H.C., Costa, D.K.: Improving long-term outcomes after sepsis. *Critical care clinics* **34**(1), 175 (2017)
- [5] Evans, L., Rhodes, A., Alhazzani, W., Antonelli, M., Coopersmith, C.M., French, C., Machado, F.R., McIntyre, L., Ostermann, M., Prescott, H.C., *et al.*: Surviving sepsis campaign: international guidelines for management of sepsis and septic shock 2021. *Critical care medicine* **49**(11), 1063–1143 (2021)
- [6] Seymour, C.W., Gesten, F., Prescott, H.C., Friedrich, M.E., Iwashyna, T.J., Phillips, G.S., Lemeshow, S., Osborn, T., Terry, K.M., Levy, M.M.: Time to treatment and mortality during mandated emergency care for sepsis. *New England Journal of Medicine* **376**(23), 2235–2244 (2017)
- [7] Giamarellos-Bourboulis, E.J., Aschenbrenner, A.C., Bauer, M., Bock, C., Calandra, T., Gat-Viks, I., Kyriazopoulou, E., Lupse, M., Monneret, G., Pickkers, P., *et al.*: The pathophysiology of sepsis and precision-medicine-based immunotherapy. *Nature immunology* **25**(1), 19–28 (2024)
- [8] Seymour, C.W., Kennedy, J.N., Wang, S., Chang, C.-C.H., Elliott, C.F., Xu, Z., Berry, S., Clermont, G., Cooper, G., Gomez, H., *et al.*: Derivation, validation, and potential treatment implications of novel clinical phenotypes for sepsis. *Jama* **321**(20), 2003–2017 (2019)
- [9] Xu, Z., Mao, C., Su, C., Zhang, H., Siempos, I., Torres, L.K., Pan, D., Luo, Y., Schenck, E.J., Wang, F.: Sepsis subphenotyping based on organ dysfunction trajectory. *Critical Care* **26**(1), 197 (2022)
- [10] Yin, C., Liu, R., Zhang, D., Zhang, P.: Identifying sepsis subphenotypes via time-aware multi-modal auto-encoder. In: *Proceedings of the 26th ACM SIGKDD International Conference on Knowledge Discovery & Data Mining*, pp. 862–872

(2020)

- [11] Xie, F., Yuan, H., Ning, Y., Ong, M.E.H., Feng, M., Hsu, W., Chakraborty, B., Liu, N.: Deep learning for temporal data representation in electronic health records: A systematic review of challenges and methodologies. *Journal of biomedical informatics* **126**, 103980 (2022)
- [12] Guo, C., Lu, M., Chen, J.: An evaluation of time series summary statistics as features for clinical prediction tasks. *BMC medical informatics and decision making* **20**, 1–20 (2020)
- [13] Groenwold, R.H.: Informative missingness in electronic health record systems: the curse of knowing. *Diagnostic and prognostic research* **4**(1), 8 (2020)
- [14] Steinhäus, H.: Sur la division des corps matériels en parties. *Bull. Acad. Pol. Sci., Cl. III* **4**, 801–804 (1957)
- [15] Xie, J., Girshick, R., Farhadi, A.: Unsupervised deep embedding for clustering analysis. In: *International Conference on Machine Learning*, pp. 478–487 (2016). PMLR
- [16] Gu, Z., Gu, L., Eils, R., Schlesner, M., Brors, B.: ” circlize” implements and enhances circular visualization in r (2014)
- [17] VanderWeele, T.J., Ding, P.: Sensitivity analysis in observational research: introducing the e-value. *Annals of internal medicine* **167**(4), 268–274 (2017)
- [18] Wilkerson, M.D., Hayes, D.N.: Consensusclusterplus: a class discovery tool with confidence assessments and item tracking. *Bioinformatics* **26**(12), 1572–1573 (2010)
- [19] Yang, B., Fu, X., Sidiropoulos, N.D., Hong, M.: Towards k-means-friendly spaces: Simultaneous deep learning and clustering. In: *International Conference on Machine Learning*, pp. 3861–3870 (2017). PMLR
- [20] Fard, M.M., Thonet, T., Gaussier, E.: Deep k-means: Jointly clustering with k-means and learning representations. *Pattern Recognition Letters* **138**, 185–192 (2020)
- [21] Tsai, P.-J., Chen, K.-F., Limbud, C., Tseng, Y.-J.: navidcn: Navigator-guided multi-modal deep clustering for sepsis phenotyping in early icu admission. In: *2025 47th Annual International Conference of the IEEE Engineering in Medicine and Biology Society (EMBC)*, pp. 1–7 (2025). IEEE
- [22] Vincent, J.-L., Moreno, R., Takala, J., Willatts, S., De Mendonça, A., Bruining, H., Reinhart, C., Suter, P., Thijs, L.G.: The sofa (sepsis-related organ failure assessment) score to describe organ dysfunction/failure: On behalf of the working

group on sepsis-related problems of the european society of intensive care medicine (see contributors to the project in the appendix). *Intensive care medicine* **22**(7), 707–710 (1996)

- [23] Lambden, S., Laterre, P.F., Levy, M.M., Francois, B.: The sofa score—development, utility and challenges of accurate assessment in clinical trials. *Critical Care* **23**, 1–9 (2019)
- [24] Yang, A., Kennedy, J.N., Reitz, K.M., Phillips, G., Terry, K.M., Levy, M.M., Angus, D.C., Seymour, C.W.: Time to treatment and mortality for clinical sepsis subtypes. *Critical Care* **27**(1), 236 (2023)
- [25] Silversides, J.A., Major, E., Ferguson, A.J., Mann, E.E., McAuley, D.F., Marshall, J.C., Blackwood, B., Fan, E.: Conservative fluid management or deresuscitation for patients with sepsis or acute respiratory distress syndrome following the resuscitation phase of critical illness: a systematic review and meta-analysis. *Intensive care medicine* **43**, 155–170 (2017)
- [26] Scheeren, T.W., Bakker, J., De Backer, D., Annane, D., Asfar, P., Boerma, E.C., Cecconi, M., Dubin, A., Dünser, M.W., Duranteau, J., *et al.*: Current use of vasopressors in septic shock. *Annals of intensive care* **9**, 1–12 (2019)
- [27] Hidalgo, D.C., Patel, J., Masic, D., Park, D., Rech, M.A.: Delayed vasopressor initiation is associated with increased mortality in patients with septic shock. *Journal of Critical Care* **55**, 145–148 (2020)
- [28] Shi, R., Hamzaoui, O., De Vita, N., Monnet, X., Teboul, J.-L.: Vasopressors in septic shock: which, when, and how much? *Annals of translational medicine* **8**(12), 794 (2020)
- [29] Pollard, T.J., Johnson, A.E., Raffa, J.D., Celi, L.A., Mark, R.G., Badawi, O.: The eicu collaborative research database, a freely available multi-center database for critical care research. *Scientific data* **5**(1), 1–13 (2018)
- [30] Yen, S.-C., Wu, C.-C., Tseng, Y.-J., Li, C.-H., Chen, K.-F.: Using time-course as an essential factor to accurately predict sepsis-associated mortality among patients with suspected sepsis. *Biomedical Journal* **47**(3), 100632 (2024)
- [31] Johnson, A.E., Bulgarelli, L., Shen, L., Gayles, A., Shammout, A., Horng, S., Pollard, T.J., Hao, S., Moody, B., Gow, B., *et al.*: Mimic-iv, a freely accessible electronic health record dataset. *Scientific data* **10**(1), 1 (2023)
- [32] Shankar-Hari, M., Phillips, G.S., Levy, M.L., Seymour, C.W., Liu, V.X., Deutschman, C.S., Angus, D.C., Rubenfeld, G.D., Singer, M., *et al.*: Developing a new definition and assessing new clinical criteria for septic shock: for the third international consensus definitions for sepsis and septic shock (sepsis-3). *Jama* **315**(8), 775–787 (2016)

- [33] Zhang, Z., Zhang, G., Goyal, H., Mo, L., Hong, Y.: Identification of subclasses of sepsis that showed different clinical outcomes and responses to amount of fluid resuscitation: a latent profile analysis. *Critical Care* **22**, 1–11 (2018)
- [34] Komorowski, M., Celi, L.A., Badawi, O., Gordon, A.C., Faisal, A.A.: The artificial intelligence clinician learns optimal treatment strategies for sepsis in intensive care. *Nature medicine* **24**(11), 1716–1720 (2018)
- [35] Moor, M., Bennett, N., Plečko, D., Horn, M., Rieck, B., Meinshausen, N., Bühlmann, P., Borgwardt, K.: Predicting sepsis using deep learning across international sites: a retrospective development and validation study. *EClinicalMedicine* **62** (2023)
- [36] Lin, B.Y., Lee, S., Khanna, R., Ren, X.: Birds have four legs?! numersense: Probing numerical commonsense knowledge of pre-trained language models. *arXiv preprint arXiv:2005.00683* (2020)
- [37] Hegselmann, S., Buendia, A., Lang, H., Agrawal, M., Jiang, X., Sontag, D.: Tabllm: Few-shot classification of tabular data with large language models. In: *International Conference on Artificial Intelligence and Statistics*, pp. 5549–5581 (2023). PMLR
- [38] Vaswani, A., Shazeer, N., Parmar, N., Uszkoreit, J., Jones, L., Gomez, A.N., Kaiser, L., Polosukhin, I.: Attention is all you need. *Advances in neural information processing systems* **30** (2017)
- [39] Rupp, M., Peter, O., Pattipaka, T.: Exbehrt: Extended transformer for electronic health records. In: *International Workshop on Trustworthy Machine Learning for Healthcare*, pp. 73–84 (2023). Springer
- [40] Ferreira, F.L., Bota, D.P., Bross, A., Mélot, C., Vincent, J.-L.: Serial evaluation of the sofa score to predict outcome in critically ill patients. *Jama* **286**(14), 1754–1758 (2001)